

COMPUTATION OF TRANSIENT VOLTAGES NEAR COMPLEX GROUNDING SYSTEMS CAUSED BY LIGHTNING CURRENTS

Leonid Grcev
Elektrotehnicki fakultet
Univezitet "Kiril i Metodij"
Karpos II bb, P.O. Box 574
YU-91000 Skopje, Yugoslavia

Abstract: Spacious and complex grounding systems are often part of a lightning protection system in industrial and power plants. Large lightning current impulses can cause large transient voltages coupled to control and signal circuits in near vicinity to the grounding systems. Two different computer programs are developed for numerical evaluation of such transient voltages. It is shown that simplifications used in previous computer models lead to erroneous results.

Introduction

Spacious grounding systems with complex configuration of electrodes are often part of the lightning protection system in industrial and power plants. The large currents that flow during a lightning impulse can cause large voltages along a path between points on or near grounding systems. These transient voltages can couple to cables, connected to or near the grounding system, which are part of the control and signal circuits. Such coupling can be a reason for the occurrence of false signals or alarms, which can cause malfunction or even destruction of important electronic instrumentation. In order to determine measures of protection of the instrumentation control circuits a more precise knowledge of the induced transient voltages is necessary.

High frequency analysis of the grounding systems is addressed in two recent papers by Takashima[1] and Papalexopoulos[2]. To avoid complications in the development of the analytical solution, different simplifying approximations are employed. The common approximation is the quasi-static assumption. As consequence, the influence of the earth's surface is taken into account by the image theory. Furthermore, Takashima[1] calculates the current distribution in the grounding system and the electric field distribution in the vicinity assuming that the electric charges on the grounding electrodes are the only sources of the electric field. Papalexopoulos[2] neglects the integration path dependent component of the voltage. These simplifying approaches, in fact, neglect the influence of the time-varying longitudinal current in the grounding electrodes, as a source of an additional component of the electric field.

The aim of this paper is to investigate the influence of this neglected component of the electric field on the analytical evaluation of the transient voltages induced in near vicinity of the grounding systems energized by injection of current impulse.

Statement of the problem

In a usual standard low frequency analysis of the grounding systems, potential distribution is calculated first and voltages are obtained next as potential differences. Since for higher frequencies voltages are not equal to the potential difference, the voltages here are calculated as a line integral of the electric field vector along a given path.

The physical model

The physical model is based on the following assumptions.

The grounding system is assumed to be a network of straight cylindrical metallic conductors with arbitrary orientation and finite conductivity. The conductors are subject to the thin-wire approximation, assuming that conductor radius is much smaller than the wavelength and the wire length is much greater than the radius. In other words, radial currents in the conductors, currents over the flat end surfaces of the conductors and the circumferential currents are neglected. In addition, azimuthal variations of the axial currents in the conductors are neglected. These assumptions enable to consider the total current in the conductors as longitudinal filamentary line current placed in the axis of the conductors. Also the axial current on the open end of the grounding electrodes is assumed to be zero. Furthermore, the whole structure of the grounding system is assumed to be embedded in the soil.

Energization is by injection of current impulse by an ideal current generator with one terminal connected to the grounding system, and the other to the ground at infinity. The influence of the connecting leads is ignored.

The soil is modeled as homogeneous half-space with plane boundary, characterized by conductivity, permittivity and permeability constants.

The physical situation is illustrated in Fig. 1.

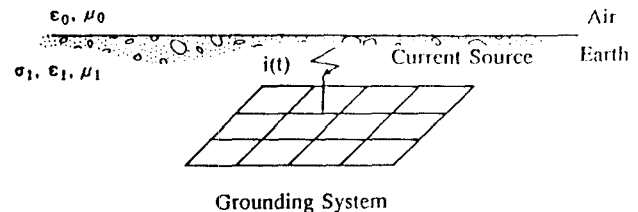


Fig. 1. Illustration of the physical situation.

The frequency-domain solution of the problem

The classical technique for the solution of the transient electromagnetic problems is employed. This involves the computation of the frequency-domain response of the structure, which is subsequently Fourier transformed to yield the desired time-domain response.

Since the main goal of this work is to investigate the influence of the longitudinal current in the grounding electrodes on the computed induced voltages, the influence of the earth's surface is taken into account by image theory, the same way as in the above mentioned simplified models.

To validate the results, two different mathematical models are solved by different numerical techniques, and the results are compared. The both are based on standard techniques from the Method of Moments (MM) (Harrington[3]). As the basis for the here developed computer programs for grounding systems analysis, two standard computer programs for antennas are used. The first one is the thin-wire program by Richmond[4] and the other is the program by Bewensee[5]. In the first case, the distribution of currents is approximated as piecewise-sinusoidal (in fact as superposition of overlapped sinusoidal dipoles, Fig. 2 (c)). The corresponding, so called, Reaction Integral Equation (RIE)

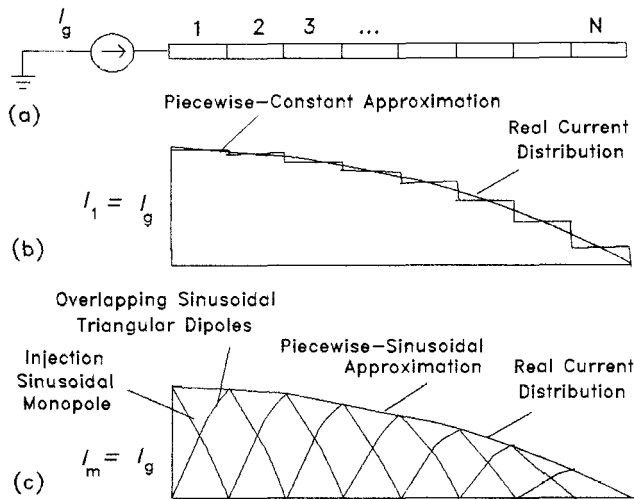


Fig. 2. (a) Segmentation of the electrode. (b) Piecewise-constant approximation of the longitudinal current. (c) Piecewise-sinusoidal approximation of the longitudinal current.

is solved by the Galerkin method. In the second case, the piecewise-constant current approximation is used, (Fig. 2.(b)), and the corresponding, so called, Mixed Potential Integral Equation (MPIE) is solved by point-matching. The details of these solutions for antennas and scatterers are available elsewhere (Harrington[3] and Richmond[6]).

In order to adapt the above antenna computer codes for grounding systems analysis, the following points are of importance:

- the ambiental medium is conducting half-space and the other half-space is air,
- the electrodes of finite conductivity are in direct contact with the conducting medium,
- the energization is by injection of current at a point in the grounding system, and
- the computer code has to be capable for computations in a range of frequencies starting from 0 Hz.

The main part of the first two points are already solved in the program by Richmond[4], since it is for thin-wire structures in unbounded conducting medium. The program by Bewensee[5] can be straightforwardly modified for unbounded conducting medium by replacing the propagation constant of the air with the corresponding of the soil. The finite conductivity of the grounding electrodes material in the program by Bewensee[5], is taken into account by the standard procedure explained in Grcev[7]. Also a subroutine for electric field evaluation is developed following the principles given in Adams[8]. The influence of the soil surface is taken into account in the both programs by the modified image theory technique Takashima[1].

The lowest frequency used was 50 Hz (which is considered equivalent to 0 Hz) and the codes are adapted for such low frequencies by conversion from SINGLE to DOUBLE PRECISION of subroutines involved in computation of the generalized impedance matrix elements.

Only the energization by injection of current requires more involved, but still straightforward modification of existing programs.

Energization by injection of current

The energization of antennas is usually modeled by a voltage applied to two closely spaced, but isolated, feed point terminals located on the exited structure or by an incident electromagnetic field illuminating the structure. The excitation by voltage can be straightforwardly modified to current following the procedure outlined in Thielle[9]. In this case, the

energization of the grounding system is modeled by the injection of a time-harmonic current in a required frequency range produced by an ideal current generator with one terminal connected to the grounding system, and the other to the ground at infinity.

Application of this model of excitation is different in the two programs.

Piecewise-constant current: Beside the usual types of segment end points: simple junction, multiple junction and open end, defined in Bewensee[5], an additional type of end point of a segment is introduced: an injection point. The current in this segment is predefined and equal to the current of the current generator.

Let the segment with an injection end point be numbered with 1, and the longitudinal current in this segment with I_1 , like in Fig. 2 (b). If I_g is the current of the current generator, then $I_1 = I_g$. Application of the MM results in generalized impedance matrix $[Z]$, which describe the electromagnetic interactions between the segments, Harrington[3]. In the process the MPIE characterizing the problem is reduced to a matrix equation of the form:

$$\begin{bmatrix} z_{22} & z_{23} & \dots & z_{2N} \\ z_{32} & z_{33} & \dots & z_{3N} \\ \vdots & \vdots & \ddots & \vdots \\ z_{N2} & z_{N3} & \dots & z_{NN} \end{bmatrix} \cdot \begin{bmatrix} I_2 \\ I_3 \\ \vdots \\ I_N \end{bmatrix} = \begin{bmatrix} -z'_{21} I_g \\ -z'_{31} I_g \\ \vdots \\ -z'_{N1} I_g \end{bmatrix} \quad (1)$$

where z_{jk} are generalized mutual impedances between the segments and I_j , $j=2,3,\dots,N$, are unknown longitudinal currents, the same as those used in antenna analysis (Harrington[3] and Bewensee[5]). The difference is in the z'_{j1} , which are the generalized mutual impedances between the injection segment (here numbered with 1) and the other segments numbered with $j=2,3,\dots,N$. The treatment is similar to the treatment of the wire open ends in Bewensee[5], but without the extended half segment with zero current. This procedure is described in detail in Grcev[10].

Piecewise-sinusoidal current: In case of the program based on the piecewise-sinusoidal current approximation, the first step is to determine the distribution of the sinusoidal dipoles, the same way as in the usual antenna case. The injection point is, in this step, treated as an ordinary wire open end. Then on the injection segment one sinusoidal monopole is added, with the terminal at the injection point, as illustrated in Fig. 2 (c). The current at the injection sinusoidal monopole terminal is equal to the current of the current generator. Let the number of the sinusoidal dipoles be equal to M . The current of the sinusoidal monopole $I_m = I_g$. Here the corresponding matrix equation has the following form:

$$\begin{bmatrix} z_{11} & z_{12} & \dots & z_{1M} \\ z_{21} & z_{22} & \dots & z_{2M} \\ \vdots & \vdots & \ddots & \vdots \\ z_{M1} & z_{M2} & \dots & z_{MM} \end{bmatrix} \cdot \begin{bmatrix} I_1 \\ I_2 \\ \vdots \\ I_M \end{bmatrix} = \begin{bmatrix} -z'_{1m} I_g \\ -z'_{2m} I_g \\ \vdots \\ -z'_{Mm} I_g \end{bmatrix} \quad (2)$$

Here z_{jk} , $j,k=1,2,\dots,M$, are mutual impedances between the M sinusoidal dipoles, and I_j , $j=1,2,\dots,M$, are unknown currents of the sinusoidal dipoles, as defined in Richmond[6]. Also here, z'_{jm} , $j=1,2,\dots,M$, are mutual impedances between the injection sinusoidal monopole designated with m , and the sinusoidal dipoles

numbered with $j=1,2,\dots,M$. The expression for the z'_{jm} can be derived from the corresponding expression in Richmond[6] for ordinary z_{jk} in a straightforward way, by defining the sinusoidal monopole as one half of an ordinary sinusoidal dipole.

Since the solution of the matrix equations (1) and (2) is straightforward with existing routines, in this way, the distribution of the longitudinal currents in the grounding system electrodes is solved in two independent ways. This is convenient for validation of the numerical results.

Electric field evaluation

The evaluation of the electric field is different for the two programs.

Piecewise-constant current: The electric field is computed by the procedure given in Adams[8]. In a compact form the expression for the electric field \vec{E} at a point can be written (Grcev[7]):

$$\vec{E} = \frac{1}{4\pi j\omega \epsilon} \sum_{n=1}^M I_n \left[(\nabla \cdot - \gamma) \int_{\Delta \ell_n} \vec{t}_n \frac{e^{-\gamma R_n}}{4\pi R_n} d\ell \right] \quad (3)$$

$$\underline{\epsilon} = \epsilon + \frac{\sigma}{j\omega}, \quad \omega = 2\pi f, \quad j = \sqrt{-1}$$

where $\Delta \ell_n$ denote the length of the n th segment and R_n is the distance from a point on $\Delta \ell_n$ to the field point. Here the vector \vec{t}_n represents the unit vector along the n th segment axis.

This form of the expression for the electric field is convenient for the analysis of the influence of the two components of the electric field. The expression in Eq. (3) is a sum of two parts: the first one is due to the charge distribution on the electrodes and the second is due to the longitudinal current in the electrodes.

The Eq. (3) is valid in homogeneous medium. In the half-space, the contribution of the image sources has to be taken into account (Takashima[1]).

Piecewise-sinusoidal current: One of the reasons for the choice of the sinusoidal dipoles for equivalent sources of the electric field is that they are probably the only finite line sources with simple closed-form expressions for the near fields (Otto[11]). The exact expressions for the electric field in the near point of a line sinusoidal monopole, in a local cylindrical coordinate system illustrated on Fig. 3, are:

$$E_\rho = \eta \frac{C}{\rho} I [-\exp(-\gamma R_2) \sinh(\gamma d) - \exp(-\gamma R_1) \cos\theta_1 - \exp(-\gamma R_2) \cos(\gamma d) \cos\theta_2] \quad (4)$$

$$E_z = \eta C I \left[-\frac{1}{R_2} \exp(-\gamma R_2) \cosh(\gamma d) - \frac{1}{R_1} \exp(-\gamma R_1) \right]$$

$$\eta = \sqrt{\frac{\mu}{\epsilon}}, \quad C = \frac{1}{4\pi \sinh(\gamma d)}$$

where various geometrical quantities are illustrated in Fig. 3. Other symbols are defined in Eq. (3). The current in the sinusoidal monopole, illustrated on Fig. 3, is zero at z_1 and have maximum with value I at z_2 .

The electric field at a point near the grounding system is the sum of contributions from the overlapping sinusoidal current monopoles in all segments. The Eq. (4) is valid in homogeneous medium. In the half-space, the contribution of the image sources have to be taken into account (Takashima[1]).

The two independent ways of computation of the

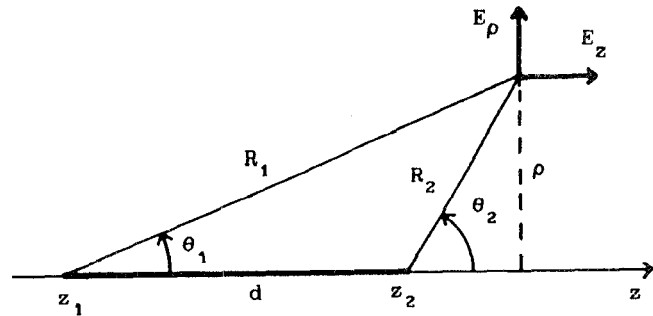


Fig. 3. Local cylindrical coordinate system.

electric field are convenient for the validation of the results.

Time-domain solution

If the electric field vector $\vec{E}(j\omega)$ at a point near the grounding system, which is a response to an injected steady-state time harmonic current $I(j\omega)$, is known for all frequencies, then the transfer function of the system $W(j\omega)$ can be simply obtained by:

$$W(j\omega) = \frac{E(j\omega)}{I(j\omega)} \quad (5)$$

where $E(j\omega)$ are components of the $\vec{E}(j\omega)$ in a appropriate coordinate system. Then the time domain solution $E(t)$ can be determined by direct application of:

$$E(t) = \mathcal{F}^{-1} \{ W(j\omega) \cdot \mathcal{F} [i(t)] \} \quad (6)$$

where $i(t)$ represents the injected current impulse at a point in the grounding system and \mathcal{F} and \mathcal{F}^{-1} are the Fourier and inverse Fourier transforms, respectively.

Since the electric field can be practically computed only for a limited number of frequencies, the discrete Fourier and inverse discrete Fourier transform are applied in the Eq. (6). Also the Fast Fourier Transform algorithm is applied for the numerical evaluation of Eq. (6) (Brigham[12]). These techniques are approximate because involve band limiting of generally unlimited functions and sampling of generally continuous functions in the time and frequency domain. It is thus necessary to determine the proper maximum values and sampling densities in frequency and time domain. Optimum values of these parameters can be usually determined after a few iterations by the convergence of the results, but the maximum value of the frequency range is also determined by the limitations of the mathematical model.

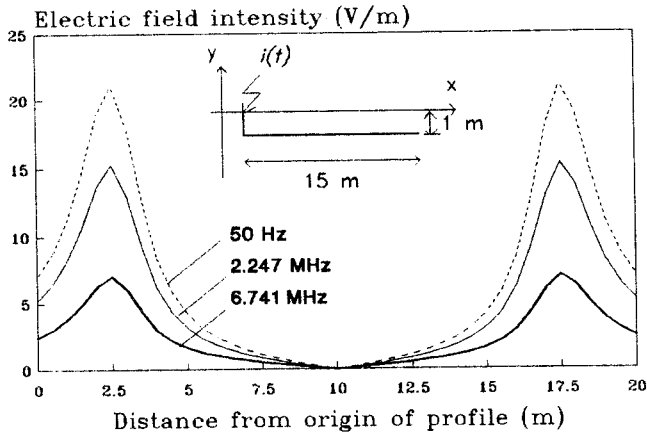
The models presented here are frequency limited due to the application of the image theory. The frequency range of the validity of the models can be determined more precisely by comparison with the more accurate model, for example (Grcev[7]). In this work the maximum frequency of around 1 MHz is adopted.

This value of the maximum frequency determines the effective cutoff frequency of the injected current impulses that can be analyzed. Faster varying impulses have higher cutoff frequency and require more accurate model.

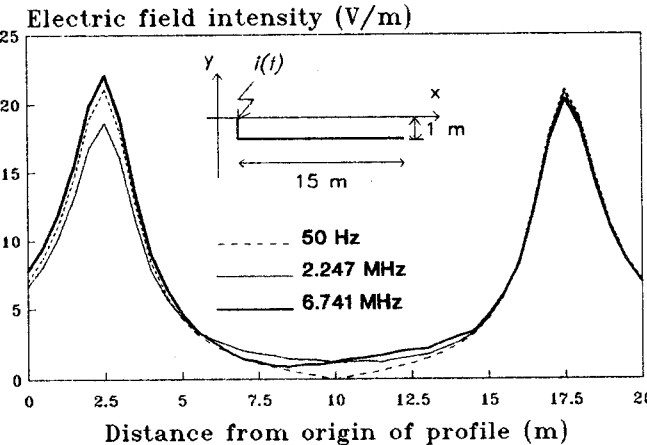
Numerical results

Comparison with previous results

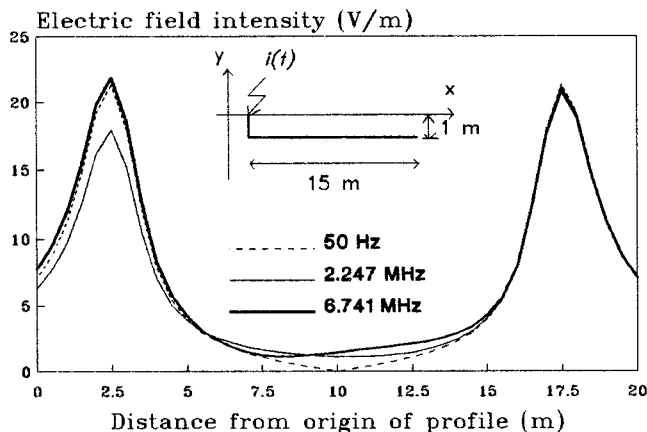
The results are compared with those given in Fig. 6 of the paper by Takashima[1]. Electric field distribution on the earth's surface above a linear electrode is computed. The electrode is 15 m long, with 0.7 cm radius, buried on 1 m depth, and of ideally conductive material. The conductance of the soil is 0.0005 mho/m



(a)



(b)



(c)

Fig. 4. Distribution of $|E_x|$ on the earth's surface.
 (a) Electric field due to charge distribution.
 (b) Complete electric field: piecewise constant current approximation. (c) Complete electric field: piecewise sinusoidal current approximation.

and the relative permittivity is 4. The energization of the electrode is by injection of time-harmonic current of $(1+j0)$ A on three frequencies: 0 Hz, 2.247 MHz and 6.741 MHz.

The results of the here developed programs for the same case as in the paper by Takashima[1], are shown in Fig. 4. Results for $|E_x|$ along the x-axis on the earth's surface above the electrode are presented.

The electrode is extended from 2.5 m to 17.5 m from the origin of the profile. The results in Fig. 4 (a) are obtained by the program based on the piecewise-constant approximation for the current, when both evaluations of the matrix elements (Eq. (1)) and electric field (Eq. (3)), are based on the reduced model for the electric field sources, that is, when electric charge distribution is assumed to be the only source of the electric field. The same model, but with complete model of the electric field sources, that is, when both the electric charges and the longitudinal currents are sources of the electric field, leads to results in Fig. 4 (b). To validate these results, the second program, based on the piecewise-sinusoidal approximation of the current, is applied to the same situation. The results are presented in Fig. 4 (c).

The results in Fig. 4 (a) are in excellent agreement with the results in the paper by Takashima[1]. They show that the values of the electric field diminish with the rise of the frequency. But when the both components of the electric field are taken into account, as in Fig. 4 (b), completely different behavior is shown. It is obvious that additional component of the electric field is added due to the time-varying longitudinal current, which is rising with the rise of the frequency, to the component of the electric field due to the electric charges. It should be noted that the first component, neglected in the models by Takashima[1] and Papalexopoulos[2], becomes dominant with the rise of the frequency. Excellent agreement of the results of the two different programs in Fig. 4 (b) and (c) validate their application for linear grounding electrodes.

Validation of the results for complex grounding systems

A 6 x 6 mesh ground mat with 10 meter square meshes buried at 0.5 meters under the earth's surface is illustrated in Fig. 5. The ground mat is assumed to be constructed from ideal conductor with radius 0.5 cm. The ideal conductors are assumed for the purpose of comparison of the results with the model equivalent to the one described in the paper by Takashima[1]. The time-harmonic current of $(1+j0)$ kA and frequency 1 MHz is injected in the vertical conductor connected to the center point of the mat. The profile on the earth's surface, along which the electric field and voltages are calculated, is given in Fig. 5 as axis x. The soil is assumed to be homogeneous with resistivity 100 ohm.m and relative permittivity 36.

Comparison of the results obtained by the two programs, one based on the piecewise-constant and the other based on the piecewise-sinusoidal approximation of the current, are presented in Fig. 6. Real and imaginary components are shown. Excellent agreement of the results validates the application of the programs for the analysis of complex grounding grids.

Results for dry and wet soil

The numerical results are presented for the electric field distributions and voltage along one profile on earth's surface for the grounding grid, defined in Fig. 5, for two typical soil conditions. One is referred as "wet soil", characterized with lower resistivity: 100 ohm.m and higher relative permittivity: 36, and the other is "dry soil", characterized with the higher value of resistivity: 1000 ohm.m and lower relative permittivity: 9.

Frequency dependence of the electric field distribution on the earth's surface for wet and dry soil is presented on Figs. 7 and 8, respectively. These results are computed by the program based on the complete electric field model. $|E_x|$ component along the

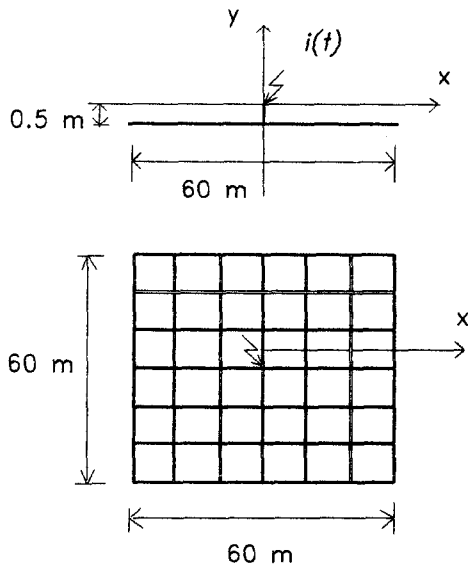


Fig. 5. Grounding grid adopted for computations.

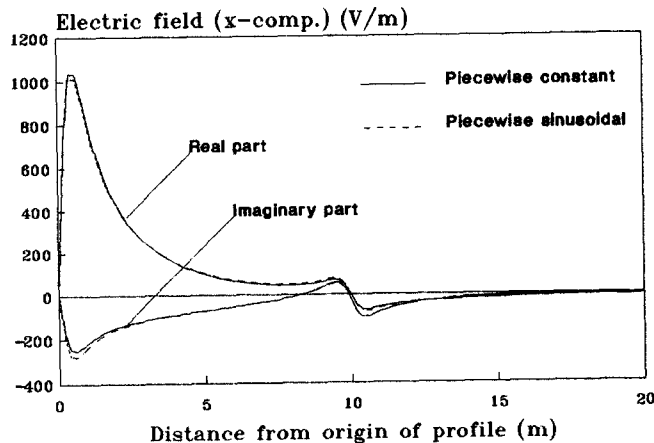


Fig. 6. Comparison of the results from the two programs: one based on the piecewise-constant and the other based on the piecewise-sinusoidal approximation of the current.

x-axis is calculated from the origin of the profile to a 40 m distant point. The profile is passing over conductor every 10 m and it ends 10 m outside the grid. For $(1+j0)$ kA time-harmonic current on 50 Hz injected in the center of the grid, electric field intensities along the profile are generally larger for dry than for wet soil about 10 times. Strong frequency dependence is shown in the vicinity to the injection point, where the values of $|E_x|$ are rising with the rise of the frequency. The area of such behavior is larger around the injecting point for dry than for wet soil. The maximum value for 1 MHz is about 30 times larger than for 50 Hz for wet soil, and about 10 times larger for dry soil.

Such frequency dependence cannot be seen when the same quantities are computed with the program based on the reduced model, that is, when the time-varying longitudinal current is neglected as a source of the electric field. The results are presented in Figs. 9 and 10, for wet and dry soil, respectively.

The amplitude spectrum of the voltages U along the profile between the points at the origin of the profile and on 40 m distance in a frequency range from 0 Hz to 1 MHz, are presented on Figs. 11 and 12, for

wet and dry soil, respectively. The results from the programs based on the complete and reduced electric field models are compared on the both figures. Again, strong frequency dependence is predicted by the complete model program. While this program predicts increase of the amplitudes of the voltages with the rise of frequencies, the reduced model program predicts completely different frequency dependence: slight decrease with rise of the frequencies. The frequency dependence is different for the wet and dry soil. For the wet soil, the rise of the amplitudes of the voltage starts intensively near the beginning of the spectrum and the rise is slowly diminishing after few hundreds kHz. For the dry soil, the rise of the amplitudes of the voltage starts on higher frequencies, larger than 100 kHz, and then the rise is constant to 1 MHz and above. This amplitude spectrum represents the transfer function of the system $H(j\omega)$ in Eq. (5).

The transient voltage responses to the excitation by standard double-exponential current impulse with maximum value 1 kA, time to maximum value 1 μ s and time to half value 50 μ s, are presented on Fig. 13 and 14, for wet and dry soil, respectively. The results from the programs based on the complete and reduced electric field models are compared on the both figures. As expected, the complete model predicts much higher values of the voltage impulse response than the reduced model. This was, of course expected from the shape of the voltage amplitude spectrum. The complete model predicts strong emphasis of the amplitudes on higher frequencies, which results in steeper fronts and higher maximum values of the voltage response. Although, the voltage responses in wet and dry soil are different, in both cases the values of the maximums of the voltage impulses predicted by the complete model are higher for about 1000 V than those predicted by the reduced model.

The dependence of the transient voltage response from the values of the front times of the injected current impulses is illustrated in Fig. 15 and 16, for wet and dry soil, respectively. In all cases the injected current impulses are double-exponential function with same maximum values 1 kA, and same time to half value 10 μ s, but different times to maximum value, 0.5 μ s, 1 μ s and 2 μ s. As expected, shorter front times of the injected current impulse results in greater values of the maximums of the transient voltage responses. Also, another process is visible from the shape of the voltage impulse for dry soil in Figs. 14 and 16. The slightly oscillatory response is due to the reflected waves from the end of the grid.

As mentioned above, the numerical computation of the transient voltage response using inverse discrete Fourier transform is an approximate process. In all presented computations the frequency spectrum of the functions was limited to 1.28 MHz. The usual logic that justify such limiting is based on the analysis of the amplitude spectrums of the typical lightning impulses, which show that frequencies higher than a few hundreds kHz are not appreciable in lightning current waves. But such analysis should be done for the amplitude spectrum of the voltage, which is the product of the current spectrum and the transfer function of the system. If the transfer function of the system is like the one illustrated in Fig. 8, the frequencies higher than a few hundreds kHz, which are not appreciable in lightning current waves, will be greatly emphasized and will become very appreciable in the transient voltage response. In such cases the limiting of the frequency spectrum of the functions at 1 MHz is no more justified. And of course, limit at 1 MHz lead to erroneous results in the early time. This is visible in Figs. 14 and 16, where the values in the early time, specially before 0.1 μ s, are greater than they should be. Numerical experiments with different maximum frequencies of the functions show that more

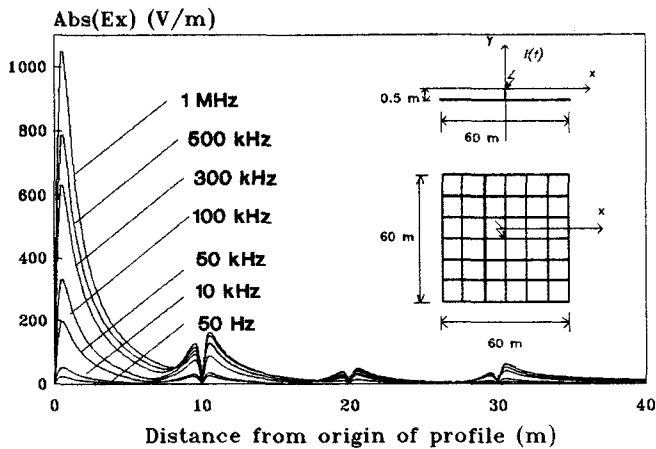


Fig. 7. Frequency dependence of $|E_x|$ on a profile on earth's surface along x-axis. Complete electric field model and wet soil.

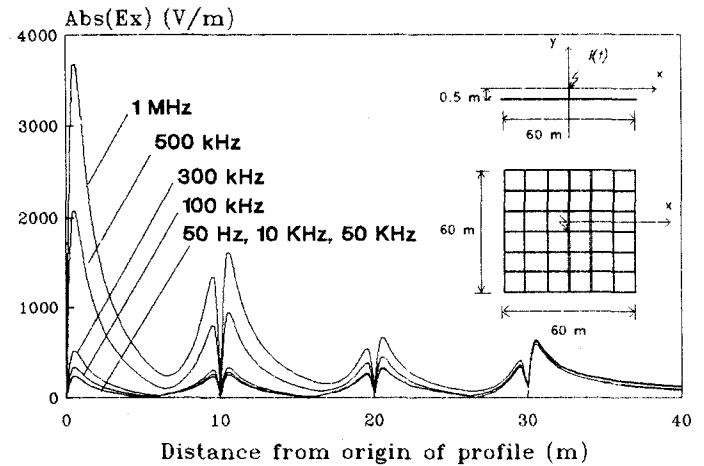


Fig. 8. Frequency dependence of $|E_x|$ on a profile on earth's surface along x-axis. Complete electric field model and dry soil.

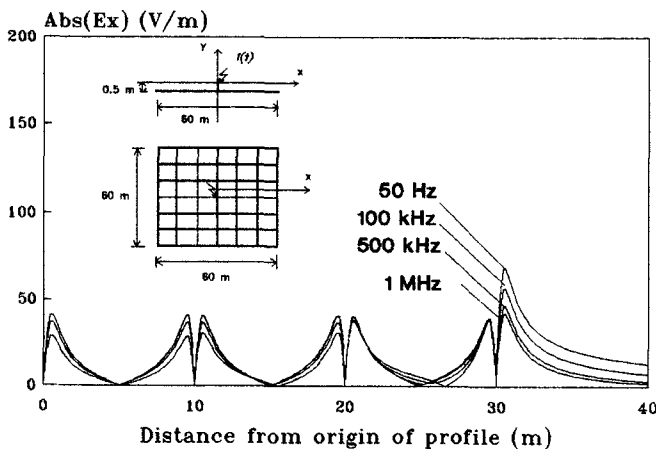


Fig. 9. Frequency dependence of $|E_x|$ on a profile on earth's surface along x-axis. Reduced electric field model and wet soil.

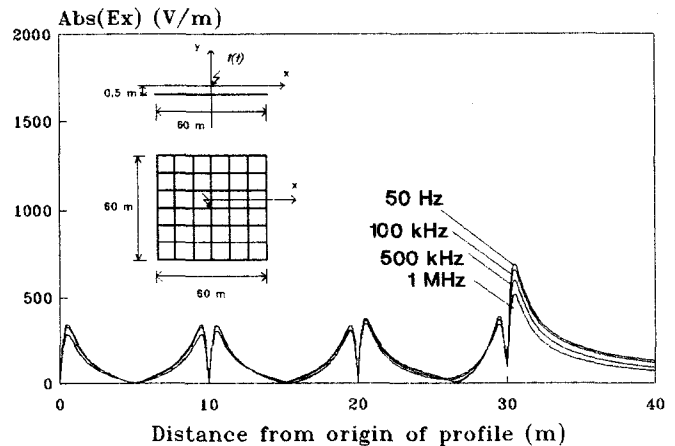


Fig. 10. Frequency dependence of $|E_x|$ on a profile on earth's surface along x-axis. Reduced electric field model and dry soil.

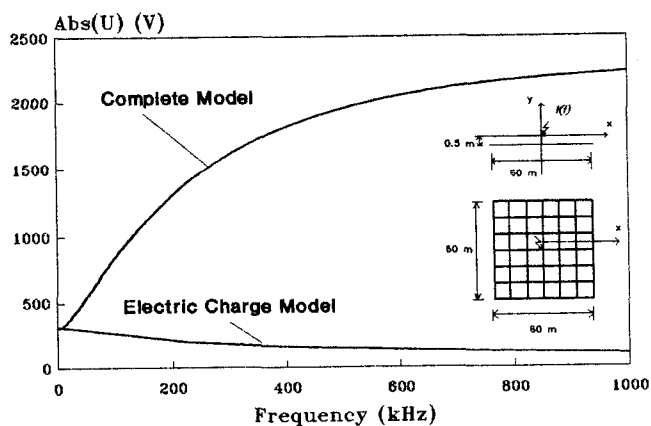


Fig. 11. Amplitude spectrum of voltages along the profile between the points in origin of profile and on 40 m distance, computed by the programs based on complete and reduced electric field models in wet soil.

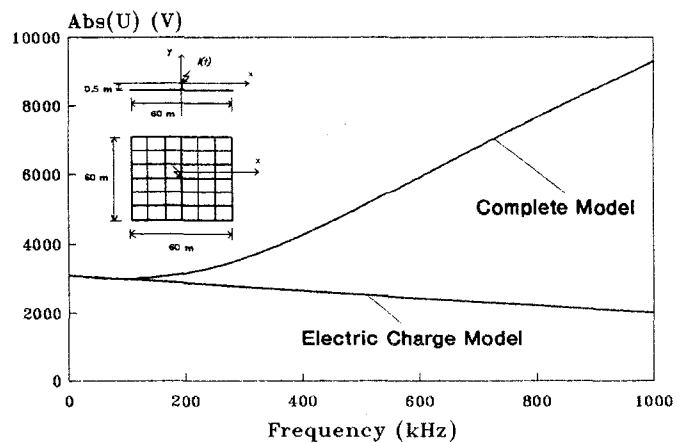


Fig. 12. Amplitude spectrum of voltages along the profile between the points in origin of profile and on 40 m distance, computed by the programs based on complete and reduced electric field models in dry soil.

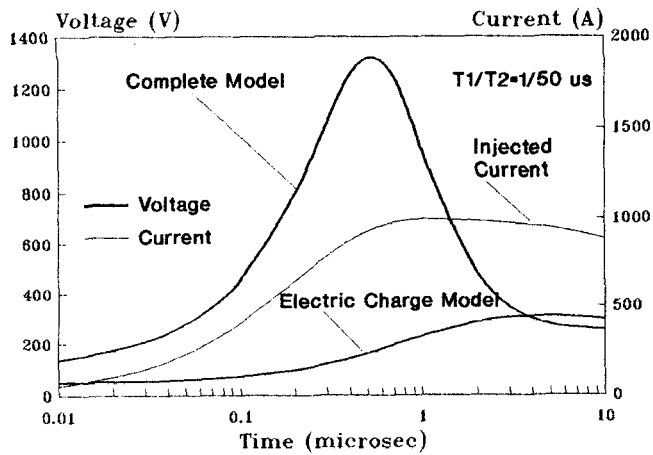


Fig. 13. Voltage response to a injected current double-exponential impulse 1 kA ($T_1/T_2 = 1\mu s/50\mu s$), computed by the programs based on complete and reduced electric field models in wet soil.

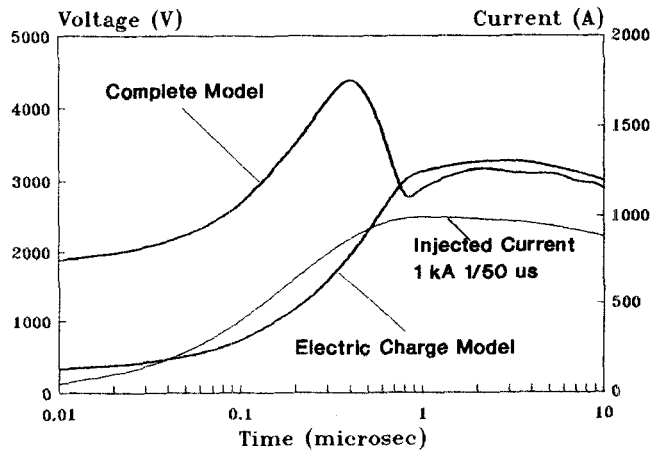


Fig. 14. Voltage response to a injected current double-exponential impulse 1 kA ($T_1/T_2 = 1\mu s/50\mu s$), computed by the programs based on complete and reduced electric field models in dry soil.

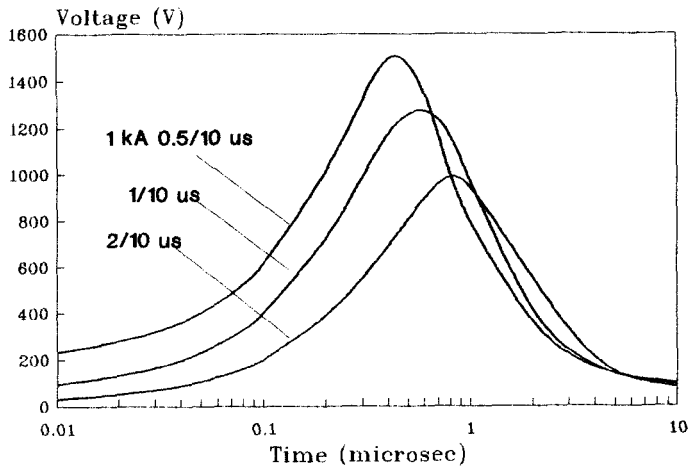


Fig. 15. Dependence of the voltage impulse response on the injected current impulse front time, computed by the program based on complete electric field model in wet soil.

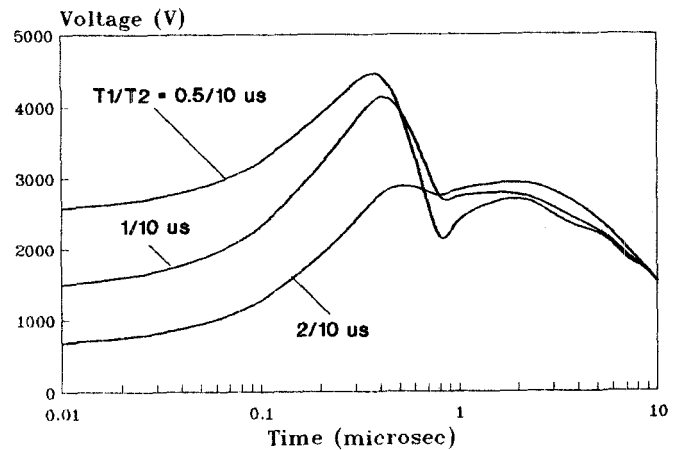


Fig. 16. Dependence of the voltage impulse response on the injected current impulse front time, computed by the program based on complete electric field model in dry soil.

accurate results can be obtained with higher values of the maximum frequencies of the functions (Grcev[7]). But in such case more accurate models, applicable on higher frequencies have to be used. That means, that instead of modeling of the earth's surface influence by image theory techniques, more accurate methods have to be used, for example, (Grcev[7]).

Conclusion

Two different computer models are developed for computation of the transient voltages in near vicinity of the complex grounding systems energized by injection of lightning current impulses. The both programs lead to results that are in excellent agreement. It is shown that previous computer models, which neglect the component of the electric field due to the time-varying longitudinal current in the grounding electrodes, erroneously predict much smaller values of the transient voltages. Also, the distribution of the voltages in the spacious and complex grounding system could not be predicted by the simplified models. It is shown that such distribution is very influenced by the position of the injection point. It should be noted

that shown results are for current impulse with maximum value of 1 kA and that lightning currents with several tens kA are possible, which can lead to much higher values of the voltages.

Some capabilities of the programs are demonstrated. It should be noted that the programs are computationally efficient enough to enable parametric analysis of spacious and complex grounding systems on general purpose computers or even on PCs. This will enable conducting of parametric studies for practical cases when protection of the instrumentation control circuits from induced transient voltages is necessary. Such parametric studies also will enable deeper insight and better understanding of the complex transient electromagnetic processes in and near grounding systems during lightning impulses.

However, the use of these programs is frequency limited to approximately 1 MHz, which in some cases limit the applicability of the programs. In such cases more accurate modeling of the influence of the earth's surface, than here applied image theory techniques, should be used.

References

- [1] T. Takashima, T. Nakae, R. Ishibashi, "High frequency characteristics of impedances to ground and field distributions of ground electrodes", IEEE Transactions on Power Apparatus and Systems, Vol. 100 pp. 1893-1900, April 1980.
- [2] A.D. Papalexopoulos, A.M. Meliopoulos, "Frequency dependent characteristics of grounding systems", IEEE Transactions on Power Delivery, Vol.2, pp. 1073-1080, October 1987.
- [3] R.F. Harrington, Field computation by moment methods, New York: Macmillan, 1968.
- [4] J.H. Richmond, "Radiation and scattering by thin-wire structures in a homogeneous conducting medium", IEEE Transactions on Antennas and Propagation, Vol. 22, p. 365, March 1974.
- [5] R.M. Bewensee, "WF-SYR/LLLL: A thin-wire computer code for antennas or scatterers with pulse expansion functions for currents", Lawrence Livermore Laboratory, Livermore, CA, Report UCRL 52028, February, 1978.
- [6] J.H. Richmond, "Radiation and scattering by thin-wire structure in the complex frequency domain", Ohio State University, Columbus, Report No. NASA CR-2396, 1974.
- [7] L. Grcev, F. Dawalibi, "An electromagnetic model for transients in grounding systems", IEEE Transactions on Power Delivery, Vol. 5, pp. 1773-1781, October 1990.
- [8] A.T. Adams, B.J. Strait, D.E. Warren, D.C. Kuo, T.E. Baldwin, "Near fields of wire antennas by matrix methods", IEEE Transactions on Antennas and Propagation, Vol. 21, pp. 602-610, September 1972.
- [9] G.A. Thielle, "Wire antennas" in R. Mittra, Editor, "Computer techniques for electromagnetics", New York: Pergamon Press, 1973, ch. 2.
- [10] L. Grcev, "Calculation of the transient impedance of grounding systems", Tech.D. thesis (in Serbo-Croat), University of Zagreb, Yugoslavia, 1986.
- [11] D.V. Otto, J.H. Richmond, "Rigorous Field Expressions for Piecewise-Sinusoidal Line Sources", IEEE Transactions on Antennas and Propagation, Vol. 17, p. 98, January 1969.
- [12] E.O. Brigham, "The Fast Fourier Transform", Englewood Hills: Prentice Hall, , 1974)